European Journal of Pharmaceutical Sciences 215 (2025) 107325

Contents lists available at ScienceDirect

European Journal of Pharmaceutical Sciences

journal homepage: www.elsevier.com/locate/ejps

Linker modifications in radiolabeled RM26-based antagonists to gastrin-releasing peptide receptor (GRPR) improved tracers' pharmacokinetics

Ekaterina Bezverkhniaia [a,*], Ayman Abouzayed [a], Panagiotis Kanellopoulos [a], Vladimir Tolmachev [b], Ulrika Rosenström [a], Anna Orlova [a,c]

[a] Department of Medicinal Chemistry, Uppsala University, 751 83 Uppsala, Sweden
[b] Department of Immunology, Genetics and Pathology, Uppsala University, 751 83 Uppsala, Sweden
[c] Science for Life Laboratory, Uppsala University, 752 37 Uppsala, Sweden

ARTICLE INFO

Keywords:
Prostate cancer
Gastrin-releasing peptide receptor
RM26
Gastrin-releasing peptide receptors (GRPR) antagonist
Linker modification
Pharmacokinetics modification

ABSTRACT

Radionuclide targeting of gastrin-releasing peptide receptor (GRPR) holds significant diagnostic and therapeutic potential, particularly in PSMA-negative/low-grade prostate cancer, estrogen receptor-positive breast cancer, and other malignancies. Recently, our group reported the development and results of the Phase I clinical evaluation of [^{99m}Tc]Tc-maSSS-PEG2-RM26, an antagonist GRPR-targeting SPECT imaging agent. This study focuses on developing the next generation of RM-26-based GRPR antagonists with enhanced metabolic stability and improved pharmacokinetics. Four new RM-26-based agents containing sarcosine (Sar) at position 11 to improve the in vivo stability and with more hydrophilic linkers were designed: Pep1 – maSSS-PEG2-[Sar^{11}]RM26, Pep2 – maSSS-PEG6-[Sar^{11}]RM26, Pep3 – maSSS-PEG2-Pip-[Sar^{11}]RM26, and Pep4 – maSSS-EEE-[Sar^{11}]RM26. These analogs were compared both in vitro and in vivo with [^{99m}Tc]Tc-maSSS-PEG2-RM26 as a reference. In PC-3 cells, [^{99m}Tc]Tc-Pep1, [^{99m}Tc]Tc-Pep2 and [^{99m}Tc]Tc-Pep3, but not [^{99m}Tc]Tc-Pep4, specifically bound to GRPR and exhibited low nanomolar affinity. When compared in vivo, [^{99m}Tc]Tc-Pep1, [^{99m}Tc]Tc-Pep2, and [^{99m}Tc]Tc-Pep3 demonstrated rapid blood clearance with different degrees of hepatobiliary excretion, particularly [^{99m}Tc]Tc-Pep2 and [^{99m}Tc]Tc-Pep3 had significantly lower activity uptake in the liver and gastrointestinal tract compared to [^{99m}Tc]Tc-maSSS-PEG2-RM26. Both [^{99m}Tc]Tc-Pep2 and [^{99m}Tc]Tc-Pep3 showed improved metabolic stability, bound specifically to GRPR in vivo, and demonstrated a tendency (not statistically significant) for higher tumor activity uptake compared to the reference peptide. Biodistribution data were confirmed by SPECT/CT imaging. In conclusion, the analogs with an elongation of the PEG2-linker either up to PEG6 (Pep2) or with the addition of a basic piperidine-containing moiety (Pep3) demonstrated an improvement of the pharmacokinetic properties of these agents and justify further investigations.

1. Introduction

The demand for personalized cancer treatment is rapidly increasing, necessitating precise characterization of tumor location, extent, and molecular profile. Imaging is crucial in the management of many cancerous malignancies, including prostate (PCa) and breast (BCa) cancers, and can be used for accurate determination of the extent of the disease, identifying areas of recurrence, and monitoring treatment response (Morgat et al., 2017; Farolfi et al., 2021). MRI and various PET tracers have been widely utilized to enhance the accuracy of conventional imaging techniques, such as CT and bone scintigraphy (Farolfi et al., 2021). For PCa, prostate-specific membrane antigen (PSMA)--targeting radioligands offer the highest diagnostic value in imaging (Perera et al., 2020), and the use of PSMA-PET is now recommended by various international guidelines for investigating PCa in different clinical settings, demonstrating clinically relevant sensitivity and specificity in the detection of metastatic lesions (Sonni et al., 2020; Hennrich and Eder, 2021; Denis et al., 2022; Zhou et al., 2022). However, PSMA

* Corresponding author.
E-mail addresses: ekaterina.bezverkhniaia@ilk.uu.se (E. Bezverkhniaia), ayman.abouzayed@ilk.uu.se (A. Abouzayed), panagiotis.kanellopoulos@ilk.uu.se (P. Kanellopoulos), vladimir.tolmachev@igp.uu.se (V. Tolmachev), ulrika.rosenstrom@ilk.uu.se (U. Rosenström), anna.orlova@ilk.uu.se (A. Orlova).

https://doi.org/10.1016/j.ejps.2025.107325
Received 13 March 2025; Received in revised form 30 September 2025; Accepted 13 October 2025
Available online 13 October 2025

exhibits significant inter- and intrapatient variability (Paschalis et al., 2019; Bakht and Beltran, 2025). This highlights the need to develop alternative tracers beyond PSMA inhibitors. The gastrin-releasing peptide receptor (GRPR) is a G-protein-coupled receptor that has been explored as a promising target for the detection and treatment of various cancer types, including PCa and BCa (Verhoeven et al., 2023; Zhang et al., 2024). In contrast to PSMA, GRPR overexpression is primarily associated with low-grade disease and has been reported in 63–100 % of PCa cases, giving it the potential to visualize PSMA-negative lesions and serve as a complementary target in the management of PCa (Verhoeven et al., 2023; Zhang et al., 2024). In BCa, the estrogen receptor (ER), progesterone receptor (PR), and human epidermal growth factor receptor 2 (HER2) are the most commonly used biomarkers in clinical practice (Hou et al., 2022). However, tumor heterogeneity remains a significant challenge in the clinical management of BCa. Both inter-tumor and intra-tumor heterogeneity imply that each BCa case could have a distinct prognosis and may require tailored therapy. As our understanding of the molecular characteristics of breast cancer grows and novel targeted therapies emerge, there is an increasing need for additional biomarkers to facilitate the development of more personalized treatment strategies (Fumagalli and Barberis, 2021). In BCa, GRPR is expressed in the primary subtypes luminal A (86 %), luminal B (70 %) and is present in 95 % of the metastatic lymph nodes. GRPR expression is strongly associated with estrogen receptor-positive cancer types, as high GRPR levels have been found in 83 % of ER-positive tumors (D'Onofrio et al., 2023; Mohseninia et al., 2025).

Over the past decade, several clinical trials have investigated imaging of GRPR expression using ^{68}Ga-labeled antagonistic peptide-based tracers, mainly suitable for PET (Mansi et al., 2021). While PET has proven efficacy and sensitivity in detecting cancers, including PCa and BCa, its limited global availability is a challenge. As a potential alternative, SPECT with ^{99m}Tc-labeled tracers shows promise. SPECT is gradually closing the gap with PET technology by significant advancements in hardware and software. Additionally, compared to ^{68}Ga available via ^{68}Ge/^{68}Ga generators, cost-effective ^{99}Mo/^{99m}Tc generators can sufficiently produce ^{99m}Tc to support daily large-scale clinical use, which makes it an attractive choice for radiopharmaceutical applications (Nawar and Türler, 2022).

There is a lack of studies on the development of GRPR imaging using ^{99m}Tc-labeled tracers. Nock et al. (2021) introduced [^{99m}Tc]Tc-DB15, a GRPR-antagonist-based radiotracer, as a potential candidate for diagnostic imaging of GRPR-positive tumors. [^{99m}Tc]Tc-DB15 was able to detect several metastatic breast cancer lesions in two patients, and now these findings need to be confirmed with further clinical studies. Vats et al. (2023) reported the synthesis and preclinical evaluation of [^{99m}Tc]Tc-HYNIC-RM2, which demonstrated a potential for further clinical translation. Our group has reported the results of a phase I clinical study on the use of [^{99m}Tc]Tc-maSSS-PEG2-RM26, which has demonstrated promising outcomes in SPECT imaging of both prostate and breast cancer (Chernov et al., 2023). [^{99m}Tc]Tc-maSSS-PEG2-RM26 was well tolerated after a single injection, allowing the visualization of primary tumors, as well as metastases, shortly after administration. However, a substantial degree of hepatobiliary excretion of [^{99m}Tc]Tc-maSSS--PEG2-RM26, detected on images, may worsen the visualization of lesions in the lower abdomen and complicate the detection of hepatic metastases, limiting its clinical application. Kidneys are considered to be an organ where tumors rarely metastasize, and since the position of the kidneys is well-defined, it is possible to distinguish a high activity accumulation in the kidneys from other organs and tissues (Decristoforo and Mather, 1999). A reduction of hepatic excretion, and thus a reduction of accumulation of activity in the gastrointestinal tract, might improve the imaging properties of ^{99m}Tc-labeled imaging agents. Our group has recently reported on a series of GRPR antagonists based on the RM26 sequence with sarcosine at position 11, D-Phe-Gln-Trp-Ala--Val-Sar-His-Sta-Leu-NH_2, and a DOTAGA chelator coupled to it via various linkers intended to modify their pharmacokinetic properties (Abouzayed et al., 2023a; Obeid et al., 2024). The introduction of [Sar^{11}] increased the peptide's in vivo stability and affinity to GRPR, thus leading to an improved tumor uptake (Abouzayed et al., 2023a). Furthermore, the increase in overall and local hydrophilicity of radiolabeled peptides usually reduces their hepatic uptake (Hosseinimehr et al., 2012). The introduction of basic residues in the linker further improved receptor affinity and enhanced the uptake in GRPR-expressing tumors in the murine model (Obeid et al., 2024). These results demonstrate that linker modification is a promising way to modulate the targeting properties and pharmacokinetic profile of the radiotracer. Therefore, we hypothesized that modulation of hydrophilicity by linker modifications might suppress hepatobiliary excretion of RM26-based tracers labeled with ^{99m}Tc as well. Taking into account literature data and our experience in tracers' design, we have synthesized four new peptides based on RM26 (Fig. 1).

As the use of a maSSS chelator enables stable coupling of ^{99m}Tc to the targeting moiety (Robu et al., 2017) and permits the formulation of labeling kits, which simplifies clinical translation (Abouzayed et al., 2023b), the chelator part was not further modified. Multiple structural interventions were made to enhance the resistance of GRPR-antagonists to the proteolytic action of proteases (Mansi et al., 2021). Thus, the first step towards pharmacokinetic modification in the present study was [Gly^{11}] substitution with [Sar^{11}]. Such alteration in [^{99m}Tc]Tc-DB15 (Nock et al., 2021), as well as in [^{111}In]In-DOTAGA-PEG2-(Sar^{11})RM26 (Abouzayed et al., 2023a), has led to high metabolic resistance to neprilysin (NEP), a major catabolizing protease of bombesin-like peptides in vivo. We have incorporated sarcosine at position 11 of maSSS-PEG2-RM26. Pep1 (maSSS-PEG2-[Sar^{11}]RM26) has a similar linker to the clinically tested maSSS-PEG2-RM26. An elongated PEG-linker was introduced in Pep2 (maSSS-PEG6-[Sar^{11}]RM26) since such modification enhanced hydrophilicity and did not negatively influence GRPR affinity (Varasteh et al., 2014). Pep3 (maSSS--PEG2-Pip-[Sar^{11}]RM26) has a similar linker as AU-RM26-M2, the agent that demonstrated the best pharmacokinetics in the above-mentioned series (Abouzayed et al., 2023a; Obeid et al., 2024). The addition of a basic group, piperidine, resulted in improved tumor uptake and optimal clearance (Obeid et al., 2024). Pep4 (maSSS-EEE-[Sar^{11}]RM26) was designed to hydrophilize the agent via a negatively charged triglutamate linker instead of PEG2. It has been reported that the introduction of glutamate residues in short proteins results in conjugates with increased hydrophilicity and lower hepatic uptake (Rosik et al., 2014; Ding et al., 2019; Garousi et al., 2022; Deyev et al., 2024).

In this study, we investigated the biological properties of four new linker-modified GRPR-targeting analogs. The designed peptides were labeled with ^{99m}Tc, and the GRPR affinity, cell uptake, in vivo metabolic stability, tumor targeting, and pharmacokinetic properties were evaluated.

2. Materials and methods

The GRPR antagonists maSSS-PEG2-RM26, Pep1, Pep2, Pep3, and Pep4 were synthesized by Pepmic Co., Ltd. (Suzhou, China) based on our molecular design. Mass spectra of Pep1, Pep2, Pep3, and Pep4 can be found in Supplementary Materials (Figures S1-S4). Prostate carcinoma cell line PC-3 (GRPR positive) was purchased from ATCC (Manassas, VA, USA) and maintained according to ATCC recommendations in RPMI-1640 media. Media supplements (fetal bovine serum, penicillin-streptomycin (100 IU/mL penicillin, 100 μg/mL streptomycin), 2 mM L-glutamine, and trypsin-EDTA solution for cell detachment were purchased from Biochrom AG (Berlin, Germany). ^{99m}Tc was obtained as [^{99m}Tc]$NaTcO_4$ by elution from a ^{99}Mo/^{99m}Tc generator (Mallinckrodt Inc., St. Louis, MO, USA). The radioactivity content in cells and organs was measured using the 2480 Wizard2TM gamma counter (PerkinElmer, Waltham, MA, USA).

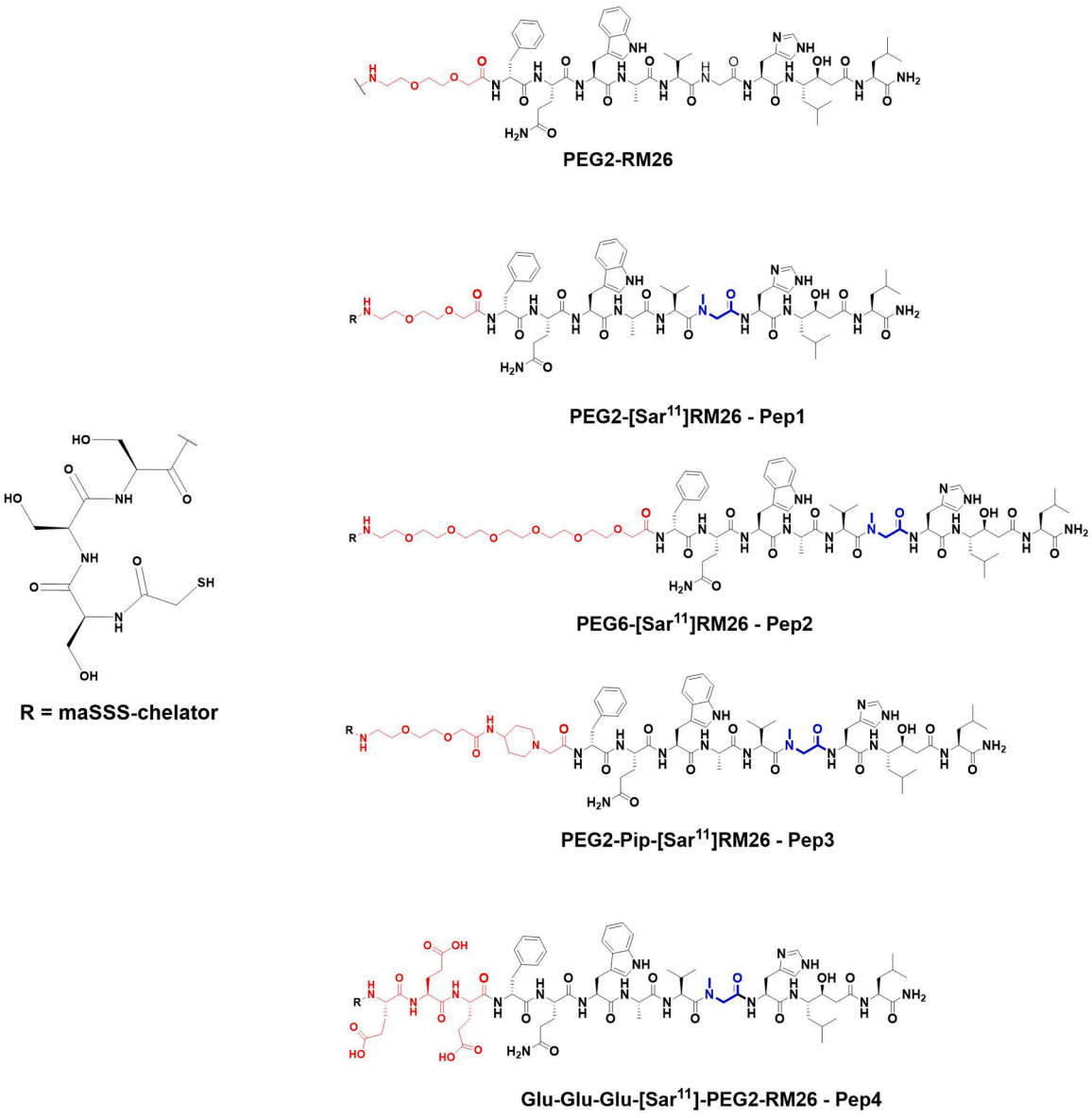

Fig. 1. Chemical structures of maSSS-PEG2-RM26, Pep1, Pep2, Pep3 and Pep4. Structural modifications are marked with colours.

2.1. Radiolabeling of GRPR antagonists and their characterization

Peptides were radiolabeled with ^{99m}Tc as previously described (Abouzayed et al., 2021). Briefly, 2 nmol of each peptide was added to a lyophilized kit containing 5 mg of gluconic acid sodium salt, 100 μg of ethylenediaminetetraacetic acid (EDTA), and 75 μg of stannous chloride. pH of the labeling solution was ~7.4. Thereafter, freshly eluted pertechnetate ([^{99m}Tc]TcO_4, up to 76 MBq) was added to the mixture, and the vial was incubated at 90 °C for 60 min. The radiochemical yield was analyzed using instant thin-layer chromatography (iTLC) strips (Agilent Technologies, Santa Clara, CA, USA) eluted with PBS ($R_f = 0$ for the radiolabeled peptide and $R_f = 1$ for ^{99m}Tc-pertechnetate and ^{99m}Tc-gluconate) and pyridine: acetic acid: water, 5:3:1.5 ($R_f = 1$ for the radiolabeled peptide and $R_f = 0$ for reduced hydrolyzed technetium colloid). iTLC was analyzed using Cyclone Plus Storage Phosphor System (PerkinElmer, Waltham, MA, USA). The reaction mixture was also analyzed according to method A on reversed-phase HPLC (Hitachi Chromaster, Luna C18 column (5 μm, 100 Å, 150 × 4.6 mm, Phenomenex, Værløse, Denmark)) with a gradient from 5 to 70 % acetonitrile (0.1 % v/v trifluoroacetic acid) in water over 15 min. To test the stability, the radiolabeled peptides were incubated with a 300 × molar excess of cysteine or with PBS at room temperature for 1 h. The octanol-water distribution coefficient (logD) was determined as previously described (Varasteh et al., 2014).

2.2. In vitro characterization

2.2.1. Cell binding and internalization of ^{99m}Tc-labeled GRPR antagonists

PC-3 cells (1×10^6) were seeded 1 day before the experiment. On the day of the experiment, a set of wells in the control group was incubated with 1 μM of NOTA-PEG_2-RM26 to pre-saturate GRPR. After 10 min at room temperature, 1 nM of each radiolabeled peptide was added and incubated at 37 °C for 1 hour. The cells were then detached by incubating with trypsin-EDTA, collected, and measured for radioactivity content on an automated gamma counter. The internalization of [^{99m}Tc]Tc-Pep1, [^{99m}Tc]Tc-Pep2, and [^{99m}Tc]Tc-Pep3 (1 nM/well) at 1, 4, and 24 h of incubation was evaluated in PC-3 cells using the acid wash method as previously described (Abouzayed et al., 2021).

2.2.2. Affinity determination

The affinity of [^{99m}Tc]Tc-Pep1, [^{99m}Tc]Tc-Pep2, and [^{99m}Tc]Tc-Pep3 towards GRPR was determined, as previously described (Abouzayed et al., 2021), by real-time measurements using LigandTracer® yellow (Ridgeview Diagnostics, Uppsala, Sweden). The assay was done on living PC-3 cells (3×10^6 cells per petri dish) at room temperature with radiolabeled peptide concentrations of 1 and 3 nM. The K_D values were determined using TraceDrawer Software (Ridgeview Instruments, Vänge, Sweden).

2.3. In vivo characterization

The in vivo experiments were carried out on BALB/c nu/nu or NMRI mice purchased from Scanbur A/S (Sollentuna, Sweden). The in vivo studies were conducted according to the guidelines of the Declaration of Helsinki and approved by the Ethics Committee for Animal Research in Uppsala, Sweden (Approval number: 5.8.18-00473/2021, 26 February 2021).

2.3.1. Biodistribution and in vivo targeting specificity of ^{99m}Tc-labeled GRPR antagonists

[^{99m}Tc]Tc-Pep1, [^{99m}Tc]Tc-Pep2, [^{99m}Tc]Tc-Pep3, and the reference GRPR antagonist [^{99m}Tc]Tc-maSSS-PEG$_2$-RM26 were evaluated in NMRI mice to compare their biodistribution profile and to select the most promising candidates to be tested in PC-3 tumor-bearing Balb/c nu/nu mice. Briefly, 30 kBq (40 pmol) of each radiotracer was injected, and each group of mice ($n = 4$) was euthanized at 3 h post-injection (pi). The organs of interest were collected, weighed, and measured for their radioactivity content.

Following the biodistribution study in NMRI mice, [^{99m}Tc]Tc-Pep2 and [^{99m}Tc]Tc-Pep3 were selected as promising candidates for further evaluation in PC-3 tumor-bearing Balb/c nu/nu mice to compare with the reference GRPR antagonist [^{99m}Tc]Tc-maSSS-PEG$_2$-RM26. Briefly, the mice were implanted with 5×10^6 PC-3 cells 4 weeks before the study. On the day of the experiment, 30 kBq (40 pmol) of each radiotracer was injected, and the mice ($n = 4$) were euthanized at 3 h pi. The organs of interest were collected, weighed, and measured for their radioactivity content.

To evaluate the in vivo targeting specificity, additional PC-3 tumor-bearing Balb/c nu/nu mice were injected with 30 kBq (40 pmol) of [^{99m}Tc]Tc-Pep2 and [^{99m}Tc]Tc-Pep3 in addition to 5 nmol of non-labeled NOTA-PEG$_2$-RM26. The mice ($n = 4$) were euthanized at 3 h pi, and the organs of interest were collected, weighed, and measured for their radioactivity content.

2.3.2. In vivo stability of ^{99m}Tc-labeled GRPR antagonists

[^{99m}Tc]Tc-Pep2 and [^{99m}Tc]Tc-Pep3 were tested in comparison with the reference [^{99m}Tc]Tc-maSSS-PEG$_2$-RM26 in NMRI mice (2 mice per peptide), 5 min after injection of 46 MBq (3 nmol) of peptide. The blood was drawn from the heart through a puncture using a cold heparinized syringe. The blood was then added to cold tubes containing 20 µl EDTA 20 mM, mixed, and centrifuged for 10 min at 2000 g at – 4 °C. Plasma was collected and diluted with acetonitrile (4 °C) in a 1:1 ratio. Samples of plasma were centrifuged for 10 min at 15.000 g at – 4 °C. The supernatant was collected and concentrated at 50 °C under a N_2 stream to V ~ 50 µl. Samples were diluted with PBS (4 °C) and kept in the fridge until HPLC analysis. Radio-HPLC analysis was performed according to method B using a Hitachi Chromaster HPLC system with a radioactivity detector and Phenomenex Luna® C18 column (100 Å; 150 × 4.6 mm; 5 µm) at room temperature (20 °C). Solvent A was 0.1 % trifluoroacetic acid (TFA) in H_2O, solvent B was 0.1 % TFA in acetonitrile, and the flow rate was 1 mL/min. For identity and purity analysis, the method with a gradient from 5 to 60 % solvent B over 20 min was used.

2.3.3. SPECT/CT imaging

PC-3 tumor-bearing Balb/c nu/nu mice were injected with 1 MBq (40 pmol) of the reference GRPR antagonist [^{99m}Tc]Tc-maSSS-PEG$_2$-RM26, [^{99m}Tc]Tc-Pep2, and [^{99m}Tc]Tc-Pep3. At 3 h pi, the mice were scanned on a NanoScan® SPECT/CT scanner (Mediso Medical Imaging Systems Ltd., Budapest, Hungary).

2.4. Data analysis

The data were analyzed using unpaired two-tailed *t*-tests via GraphPad Prism 8 for Windows (GraphPad Software, San Diego, CA, USA). P-values <0.05 indicated significant differences.

3. Results

3.1. Radiolabeling and in vitro assays

All four peptides were radiolabeled with sufficient radiochemical yields (> 95 %) determined by radio-iTLC. RHT was <0.5 %. To cross-validate radio-iTLC data, radio-HPLC analysis (Method A) was performed (Supplementary Materials Figure S5) and confirmed the results of iTLC analysis. There was minimal release of free ^{99m}Tc after competition with a 300 times excess of cysteine in PBS (< 5 %), determined by radio-iTLC. No further purification was performed for in vitro and in vivo studies.

The in vitro cell binding specificity (Fig. 2 A, C and E) demonstrated high GRPR specificity for [^{99m}Tc]Tc-Pep1, [^{99m}Tc]Tc-Pep2, and [^{99m}Tc]Tc-Pep3 when tested on PC-3 cells. [^{99m}Tc]Tc-Pep4 showed extremely low binding to cells (<0.25 % of added activity) and no significant difference ($p = 0.45$) in cell uptake between pre-saturated GRPR and unsaturated receptors. Thus, [^{99m}Tc]Tc-Pep4 was excluded from further evaluation. The internalization of [^{99m}Tc]Tc-Pep1, [^{99m}Tc]Tc-Pep2, and [^{99m}Tc]Tc-Pep3 (Fig. 2B, D, and F) reached its maximum at 4 h of incubation and was slowly decreasing up to 24 h of incubation.

The logD values for [^{99m}Tc]Tc-Pep2 (–1.36 ± 0.01) and [^{99m}Tc]Tc-Pep3 (–1.08 ± 0.01) were lower than for [^{99m}Tc]Tc-Pep1 (–0.88 ± 0.01). The affinity measurements of [^{99m}Tc]Tc-Pep1, [^{99m}Tc]Tc-Pep2, and [^{99m}Tc]Tc-Pep3 demonstrated the best fitting with a 1:2 kinetic binding model in TraceDrawer software, revealing two equilibrium dissociation constants (K_D) in the low nanomolar range (Table 1). The LigandTracer sensorgrams of [^{99m}Tc]Tc-Pep1, [^{99m}Tc]Tc-Pep2, [^{99m}Tc]Tc-Pep3, and [^{99m}Tc]Tc-Pep4 can be found in Supplementary Materials (Figures S6-S9).

3.2. In vivo evaluation

3.2.1. Biodistribution and in vivo targeting specificity of ^{99m}Tc-labeled GRPR antagonists

The biodistribution of [^{99m}Tc]Tc-maSSS-PEG$_2$-RM26, [^{99m}Tc]Tc-Pep1, [^{99m}Tc]Tc-Pep2, and [^{99m}Tc]Tc-Pep3 was compared in NMRI mice at 3 h pi. All tested tracers demonstrated fast background clearance for all peptides, with values for blood activity concentration being below 1 %IA/g at 3 h pi (Fig. 3, Table S1). The excretion of radiolabeled peptides was predominantly via the hepatobiliary system, which manifested in elevated activity uptake in the gastrointestinal tract. However, new peptides demonstrated reduced activity uptake in the gastrointestinal tract compared to [^{99m}Tc]Tc-maSSS-PEG$_2$-RM26. [^{99m}Tc]Tc-Pep2 had 1.3-fold reduction and [^{99m}Tc]Tc-Pep3 had 1.4-fold reduction. Moreover, new peptides had significantly reduced activity uptake in the liver. [^{99m}Tc]Tc-Pep1 had 2.3-fold reduction, [^{99m}Tc]Tc-Pep2 had 10-fold reduction and [^{99m}Tc]Tc-Pep3 reduced triple compared to [^{99m}Tc]Tc-maSSS-PEG$_2$-RM26. A significant increase in kidney activity uptake was demonstrated for [^{99m}Tc]Tc-Pep1 (2.3-fold) and [^{99m}Tc]Tc-Pep3 (3.8-fold) compared with the reference peptide. Elevated uptake in the pancreas (GRPR-expressing organ) was the highest for [^{99m}Tc]Tc-Pep3, followed by [^{99m}Tc]Tc-Pep1. [^{99m}Tc]Tc-Pep1 was excluded from further evaluation as it demonstrated less potential for improvement.

The biodistribution in PC-3 tumor-bearing mice (Fig. 4 and Table S2

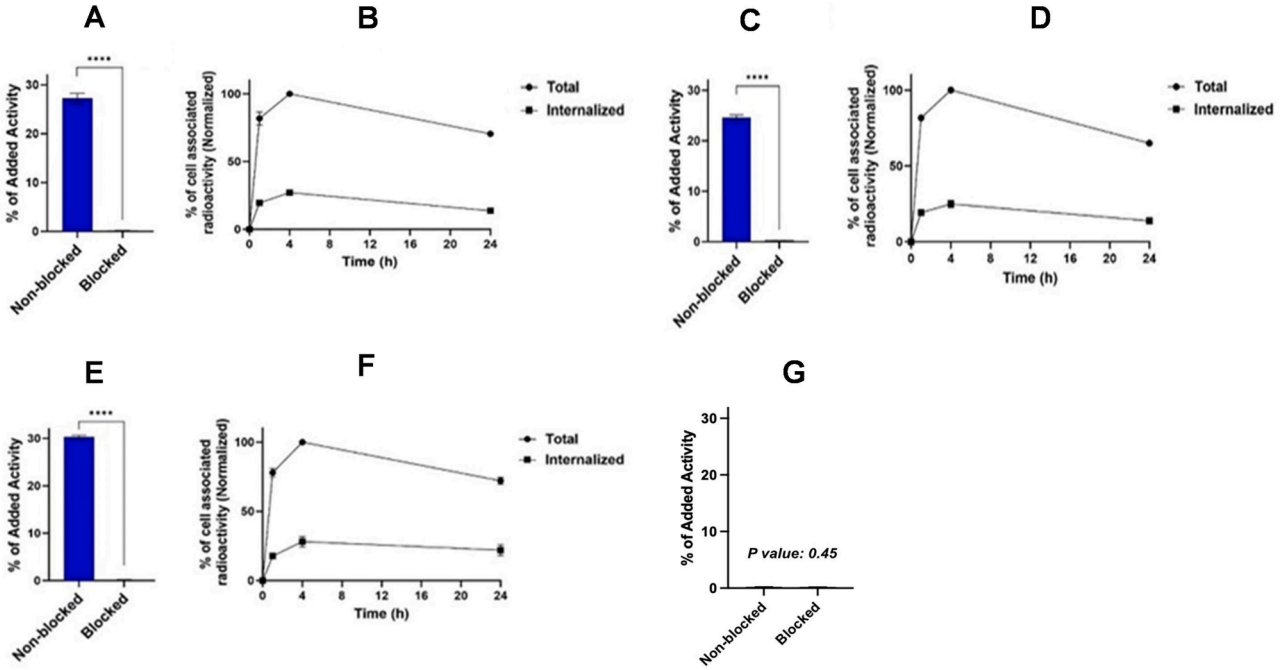

Fig. 2. The in vitro specificity test results of [^{99m}Tc]Tc-Pep1 (A), [^{99m}Tc]Tc-Pep2 (C), [^{99m}Tc]Tc-Pep3 (E), and [^{99m}Tc]Tc-Pep4 (G) done on PC-3 cells. The bars represent the mean, and the error bars indicate the standard deviation. **** denote a P value <0.0001. The internalization assay results, done on PC-3 cells, are presented for [^{99m}Tc]Tc-Pep1 (B), [^{99m}Tc]Tc-Pep2 (D), and [^{99m}Tc]Tc-Pep3 (F). The error bars represent the standard deviation.

Table 1
The equilibrium dissociation constants (K_D) of [^{99m}Tc]Tc-Pep1, [^{99m}Tc]Tc-Pep2, and [^{99m}Tc]Tc-Pep3.

Construct	K_{D1}	K_{D2}
[^{99m}Tc]Tc-maSSS-PEG2-RM26	0.06 nM*	1.2 nM*
[^{99m}Tc]Tc-Pep1	0.07 ± 0.01 nM	1.2 ± 0.3 nM
[^{99m}Tc]Tc-Pep2	1.3 ± 0.4 nM	2.5 ± 0.8 nM
[^{99m}Tc]Tc-Pep3	0.25 ± 0.02 nM	2.3 ± 0.2 nM
[^{99m}Tc]Tc-Pep4	non-measurable	

* Abouzayed et al., 2021.

that includes results of statistical analyses) showed tumor uptake of 10.9 ± 0.4 %IA/g for [^{99m}Tc]Tc-Pep2, 12 ± 2 %IA/g for [^{99m}Tc]Tc-Pep3, and 9 ± 2 %IA/g for [^{99m}Tc]Tc-maSSS-PEG$_2$-RM26; there was no significant difference between the values ($p > 0.05$, $n = 4$). [^{99m}Tc]Tc-Pep2 and [^{99m}Tc]Tc-Pep3 demonstrated 1.3-fold and 1.5-fold reduction of the gastrointestinal tract uptake compared to the reference peptide. [^{99m}Tc]Tc-Pep3 had 4.3-fold increased kidney uptake compared to [^{99m}Tc]Tc-maSSS-PEG$_2$-RM26. Tumor-to-organ ratios are presented in Table S3 (includes results of statistical analyses). Compared to [^{99m}Tc]Tc-maSSS-PEG$_2$-RM26, [^{99m}Tc]Tc-Pep2 demonstrated 2.3-fold higher tumor-to-pancreas, 1.8-fold higher tumor-to-stomach and 1.6-fold lower tumor-to-kidneys ratios. [^{99m}Tc]Tc-Pep3 had 3.2-fold lower tumor-to-kidneys ratio compared to [^{99m}Tc]Tc-maSSS-PEG$_2$-RM26.

The in vivo targeting specificity study for [^{99m}Tc]Tc-Pep2 and [^{99m}Tc]Tc-Pep3 (Fig. 5, Table S4) displayed a significant reduction of pancreatic uptake upon blocking of GRPR: 3.9 ± 0.8 %IA/g vs 0.5 ± 0.1 %IA/g and 11 ± 3 %IA/g vs 4.2 ± 0.6 %IA/g, respectively. A similar pattern was observed for PC-3 tumor uptake (10.9 ± 0.4 %IA/g vs 1.0 ± 0.3 %IA/g for [^{99m}Tc]Tc-Pep2 and 12 ± 2 %IA/g vs 3.5 ± 0.2 %IA/g for [^{99m}Tc]Tc-Pep3).

3.2.2. *In vivo stability of ^{99m}Tc-labeled GRPR antagonists*

The in vivo stability of [^{99m}Tc]Tc-Pep2 and [^{99m}Tc]Tc-Pep3 compared to [^{99m}Tc]Tc-maSSS-PEG$_2$-RM26 in peripheral mouse blood was assessed at 5 min pi via HPLC analysis (Method B) of blood plasma

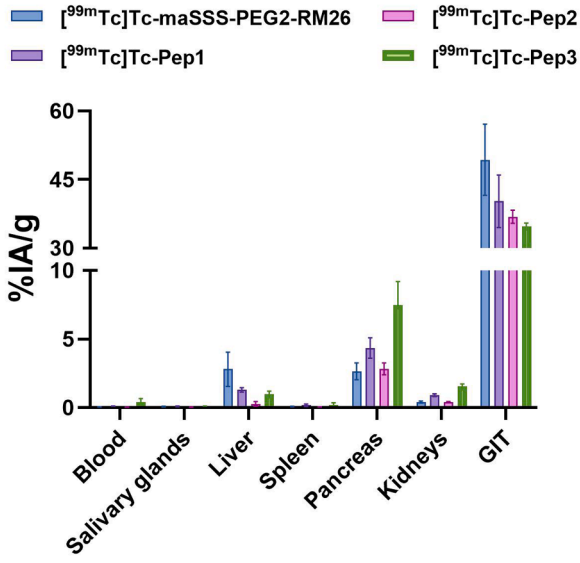

Fig. 3. The biodistribution comparison of the reference GRPR antagonist [^{99m}Tc]Tc-maSSS-PEG$_2$-RM26 and [^{99m}Tc]Tc-Pep1, [^{99m}Tc]Tc-Pep2, and [^{99m}Tc]Tc-Pep3 in NMRI mice at 3 h pi. The bars represent the mean value, and the error bars represent the standard deviation. The GIT values are presented as the %IA per whole sample.

samples. Representative radiochromatograms of radiolabeled peptides before injections, as well as blood plasma samples, are shown in Fig. 6 (details in Table S5), revealing improved stability of both [^{99m}Tc]Tc-Pep2 (≈ 62 % of intact radiopeptide) and [^{99m}Tc]Tc-Pep3 (≈ 73 % of intact radiopeptide) compared with [^{99m}Tc]Tc-maSSS-PEG$_2$-RM26 (≈ 31 % of intact radiopeptide).

3.2.3. *SPECT/CT imaging*

SPECT/CT images (Fig. 7) were in good agreement with the biodistribution profiles of [^{99m}Tc]Tc-Pep2 and [^{99m}Tc]Tc-Pep3 compared

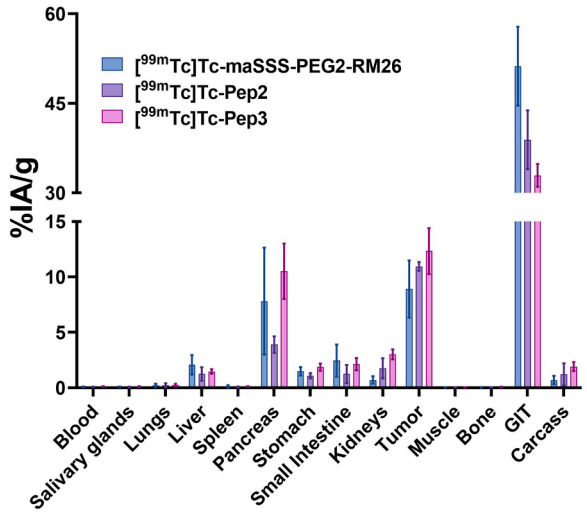

Fig. 4. The biodistribution comparison of the reference GRPR antagonist [^{99m}Tc]Tc-maSSS-PEG$_2$-RM26 with [^{99m}Tc]Tc-Pep2 and [^{99m}Tc]Tc-Pep3 in PC-3 tumor-bearing Balb/c nu/nu mice at 3 h pi. The bars represent the mean value, and the error bars represent the standard deviation. The GIT and carcass values are presented as the %IA per whole sample.

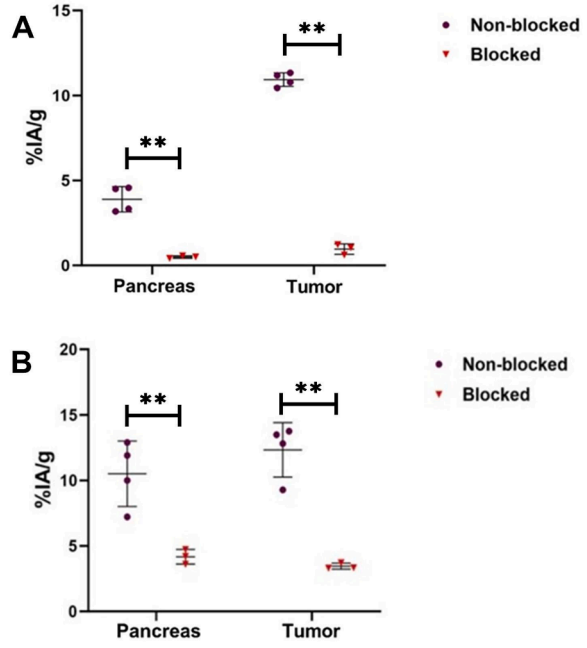

Fig. 5. The in vivo GRPR binding specificity of [^{99m}Tc]Tc-Pep2 (A) and [^{99m}Tc]Tc-Pep3 (B) in PC-3 tumor-bearing Balb/c nu/nu mice at 3 h pi. The data represent the mean value, and the error bars indicate the standard deviation. ** indicates a p-value <0.05 in a 2-tailed *t*-test.

to [^{99m}Tc]Tc-maSSS-PEG$_2$-RM26. Imaging displayed a clear visualization of the GRPR-positive tumors and pronounced activity uptake in the hepatobiliary system.

4. Discussion

The use of PSMA-PET has become a standard tool in the initial staging and detection of biochemical recurrence in high-risk PCa patients. However, its effectiveness in detecting low-grade tumor lesions is limited, as it may miss up to 15 % of lesions due to that some prostate adenocarcinomas and neuroendocrine-differentiated PCa cells do not express PSMA (Schollhammer et al., 2023). To create a more comprehensive imaging approach for PCa, it is essential to target biomarkers beyond PSMA. In this context, GRPR has emerged as a promising target (Mansi et al., 2021). GRPR is overexpressed in various malignant tumors originating from different anatomical sites, including the prostate, breast, lung, and gastrointestinal tract. Elevated GRPR expression has been particularly noted in lower-grade PCa cases (Baratto et al., 2020). Thus, GRPR holds significant diagnostic and therapeutic potential, particularly in PSMA-negative and low-grade prostate malignancies, and can serve as a complement to PSMA imaging probes in PCa. GRPR expression in BCa is associated with ER expression, particularly in luminal BCa, both in primary lesions and also in lymph nodes and distant metastasis. Thus, GRPR-targeting radiotracers also have the potential to enhance diagnostic performance and may improve clinical decision-making in BCa (D'Onofrio et al., 2023).

Our group has recently developed the GRPR-targeting tracer [^{99m}Tc]Tc-maSSS-PEG2-RM26, which demonstrated promising outcomes in both PCa and BCa SPECT imaging in a phase I clinical study (Chernov et al., 2023). However, the pharmacokinetic profile of [^{99m}Tc]Tc-maSSS-PEG2-RM26 needs to be optimized to lower the extent of hepatobiliary excretion and the resulting undesirable activity accumulation in the abdominal area, which might lead to false-positive results due to the formation of «hot» spots on images in PCa patients and also lead to undetected liver metastases in BCa patients. Several studies have investigated the influence of linkers, chelators, and/or radiometals on the pharmacology of bombesin-like peptides, highlighting the importance of selecting the optimal combination of these factors to obtain diagnostic and therapeutic radiopeptides with high potential for clinical translation (Brans et al., 2010; Abiraj et al., 2011; Jamous et al., 2014; Maina et al., 2017). In general, linker modifications seem to be one of the most promising tools in the design of new GRPR-directed agents, as a linker change can prolong tumor retention, improve serum stability, and act as a pharmacokinetic modifier (Maina et al., 2017).

In this study, we integrated the experience on structure-properties relationships to improve the pharmacokinetic behavior of the promising SPECT tracer [^{99m}Tc]Tc-maSSS-PEG2-RM26. Building on previously published studies on GRPR antagonists, we synthesized four novel radiotracers containing hydrophilic linkers (Fig. 1). All four radiopeptides were successfully labeled with ^{99m}Tc through a single-step labeling procedure. The high [^{99m}Tc]Tc(O) complex stability was verified in vitro in cysteine challenge, which is a surrogate for an in vivo stability assay (Hnatowich et al., 1994). Low values of activity uptake in the salivary gland (the indicator organ for free ^{99m}Tc) demonstrated high complex stability in vivo and are corroborated by in vitro results. [^{99m}Tc]Tc-Pep1, [^{99m}Tc]Tc-Pep2, and [^{99m}Tc]Tc-Pep3 exhibited GRPR-mediated binding to GRPR-expressing PC-3 cells with low nanomolar affinity and retained their antagonistic properties, manifested by the slow internalization profile (see Fig. 2 and Table 1). It should be noted that none of the structural modifications in [^{99m}Tc]Tc-Pep1, [^{99m}Tc]Tc-Pep2, or [^{99m}Tc]Tc-Pep3 demonstrated a negative effect on GRPR affinity, as the K_D values reflected preserved affinity in the low nanomolar range, similar to the reference peptide [^{99m}Tc]Tc-maSSS--PEG$_2$-RM26. However, the incorporation of negatively charged glutamate residues in [^{99m}Tc]Tc-Pep4 led to the loss of specific binding to GRPR, as shown in the in vitro specificity assay (see Fig. 2). It has previously been reported that positively charged bombesin analogs exhibit higher affinity to GRPR, while negative charges decrease affinity (Abiraj et al., 2011). Based on this, the use of the triglutamate-linker in the present study might be considered controversial due to the incorporation of multiple negative charges. However, it has been reported that the incorporation of a single negatively charged glutamic acid might not only hydrophilize the whole construct but also increase the retention of internalized activity in the tumor compared to the introduction of multiple negative charges (García Garayoa et al., 2008). The influence of negative charge in the linker on the affinity to GRPR might be further studied using agents with mono- and di-charged linkers. Thus, [^{99m}Tc]

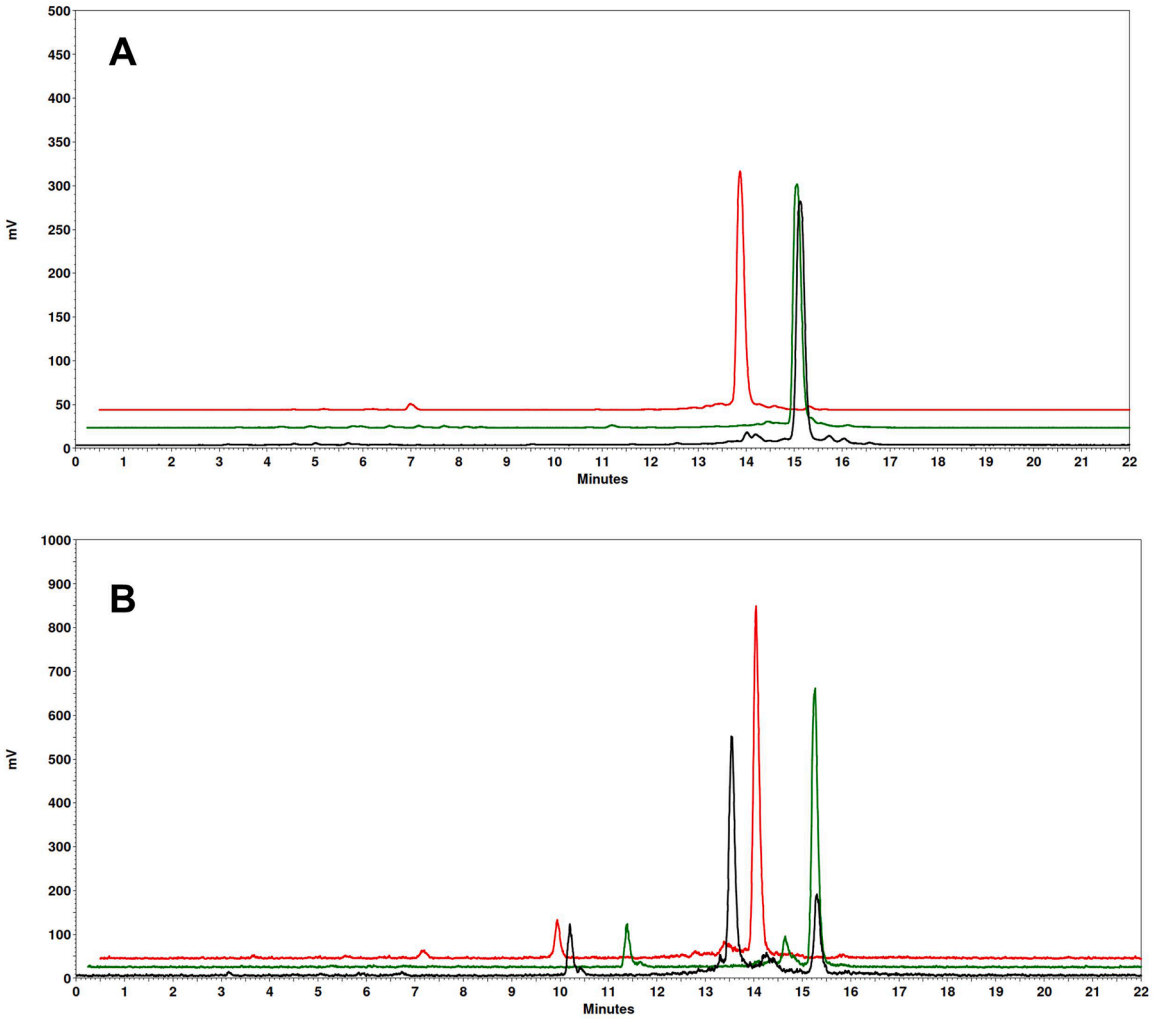

Fig. 6. Radio-HPLC chromatograms of [^{99m}Tc]Tc-maSSS-PEG$_2$-RM26 (in black), [^{99m}Tc]Tc-Pep2 (in green), [^{99m}Tc]Tc-Pep3 (in red), analyzed with method B: labeling solution before injections (**A**) and blood plasma sample analysis 5 min pi (**B**).

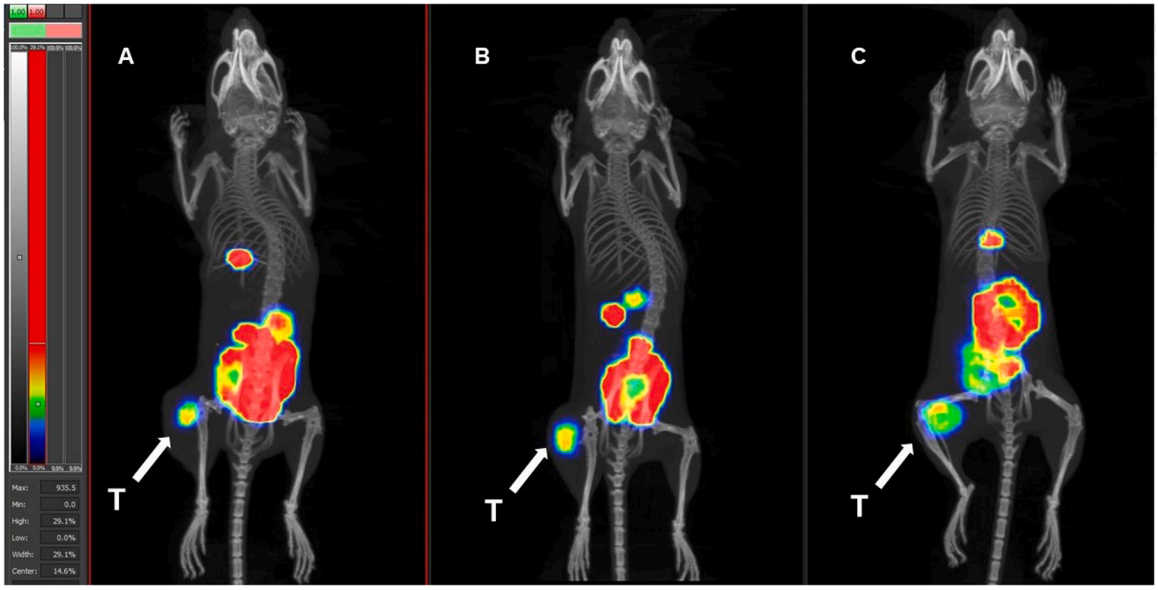

Fig. 7. The SPECT/CT images of [^{99m}Tc]Tc-maSSS-PEG$_2$-RM26 (A) and [^{99m}Tc]Tc-Pep2 (B), and [^{99m}Tc]Tc-Pep3 (C) at 3 h pi in PC-3 tumor-bearing Balb/c nu/nu mice. The white arrows (T) point to the tumors.

Tc-Pep4 was excluded from further evaluation.

The biodistribution of [^{99m}Tc]Tc-Pep1, [^{99m}Tc]Tc-Pep2, [^{99m}Tc]Tc-Pep3, and the reference construct [^{99m}Tc]Tc-maSSS-PEG$_2$-RM26 was directly compared in NMRI mice to investigate which structural modifications are advantageous for the pharmacokinetic profile (see Fig. 3). All tracers demonstrated rapid blood clearance, while the different degrees of hepatobiliary excretion manifested with pronounced activity uptake in the gastrointestinal tract. The GRPR structure in tumor tissue and normal pancreatic tissue is similar, and the receptor has a highly specific binding site, but the number and density of receptors are significantly lower in the pancreas than in tumors (Hajri et al., 1996). In an in vivo specificity assay, elevated activity uptake of [^{99m}Tc]Tc-Pep2 and [^{99m}Tc]Tc-Pep3 in the pancreas was GRPR-mediated due to physiological GRPR expression, as its blockability was demonstrated with the injection of an excess of NOTA-PEG2-RM26 (Fig. 5). As hypothesized, the incorporation of additional PEG-groups in [^{99m}Tc]Tc-Pep2 or piperidine moiety in [^{99m}Tc]Tc-Pep3 led to an increased hydrophilicity of the peptides. This was also reflected in the octanol-water coefficient values and resulted in biodistribution profiles of the peptides with reduced activity uptake in the gastrointestinal tract. [^{99m}Tc]Tc-Pep2, demonstrating the lowest LogD value (–1.36 ± 0.01) among tested peptides, has shown a 10-fold reduction of hepatic activity uptake and 1.3-fold reduction of activity uptake in the gastrointestinal tract (Fig. 3) compared to reference [^{99m}Tc]Tc-maSSS-PEG$_2$-RM26 with LogD value –0.6 ± 0.01 (Abouzayed et al., 2021). This reduction of hepatobiliary excretion for [^{99m}Tc]Tc-Pep2 was not accompanied by an increase in activity uptake in the kidneys. However, [^{99m}Tc]Tc-Pep3 has shown 3.8-fold increased kidney activity uptake together with reduced hepatobiliary excretion compared to reference [^{99m}Tc]Tc-maSSS--PEG$_2$-RM26. This may be attributed to the better plasma stability of [^{99m}Tc]Tc-Pep3 among the tested tracers, as the stable peptide fraction remains intact in circulation longer and might be more efficiently filtered in the renal tubules. This might result in reabsorption and retention of radiopeptide by the megalin/cubilin complex, a scavenger protein receptor which is involved in renal reabsorption of a large variety of ligands such as binding proteins, hormones, drugs, toxins, and enzymes (Melis et al., 2005). Importantly, it is worth noting that most ^{99m}Tc-labeled tracers exhibit safe dosimetry profiles and are not associated with renal toxicity in clinical practice. ^{99m}Tc-labeled agents are widely regarded as having among the lowest effective doses for diagnostic imaging investigations (Mattsson, 2015).

The incorporation of [Sar^{11}] in [^{99m}Tc]Tc-Pep1 did not lead to significant changes in biodistribution, thus, it was excluded from further evaluation. The improvement of the pharmacokinetic profile of [^{99m}Tc]Tc-Pep2 and [^{99m}Tc]Tc-Pep3 is not prominent compared to the reference peptide, but there is a clear indication that linker hydrophilization is a promising way to refine the biodistribution profile. [^{99m}Tc]Tc-Pep2 and [^{99m}Tc]Tc-Pep3 were then tested in mice bearing PC-3 xenografts in comparison with [^{99m}Tc]Tc-maSSS-PEG$_2$-RM26 to evaluate tumor targeting properties (see Fig. 4). Linker modification did not dramatically influence GRPR targeting properties. Slightly compromised affinity of [^{99m}Tc]Tc-Pep2 and [^{99m}Tc]Tc-Pep3 towards GRPR in comparison with [^{99m}Tc]Tc-maSSS-PEG$_2$-RM26 (Abouzayed et al., 2021) did not lead to a reduction of tumor uptake, which could be due to improved neprilysin (NEP) stability (see Fig. 6) by the [Sar^{11}] modification done, as our group has also demonstrated in the previous studies (Obeid et al., 2024). Improved in vivo stability of [^{99m}Tc]Tc-Pep2 and [^{99m}Tc]Tc-Pep3 compared to the reference [^{99m}Tc]Tc-maSSS-PEG$_2$-RM26, demonstrated a positive but minor impact on tumor targeting, and more structural modifications are needed to further improve the metabolic stability. There was a tendency, although not statistically significant, for higher tumor uptake of [^{99m}Tc]Tc-Pep2 and [^{99m}Tc]Tc-Pep3 compared to [^{99m}Tc]Tc-maSSS-PEG$_2$-RM26. Better affinity to GRPR for [^{99m}Tc]Tc-Pep3 led to higher pancreatic activity uptake and higher tumor uptake compared to [^{99m}Tc]Tc-Pep2. There was no distinguished influence on tumor-to-organ ratios among the tested constructs (see Table S3). Both [^{99m}Tc]Tc-Pep2 and [^{99m}Tc]Tc-Pep3 displayed high in vivo GRPR specificity, as shown by the significant decrease of GRPR-mediated uptake in tumors and pancreas after the co-injection of an excess of NOTA-PEG2-RM26 (see Fig. 5). The results of the in vivo biodistribution assays were verified with SPECT/CT images (see Fig. 7).

In the present study, we have demonstrated a positive effect of the incorporation of [Sar^{11}] and that the elongation of the PEG chain or introduction of the PEG2-pip linker between the chelating amino acids and GRPR-targeting moiety improved tumor targeting, metabolic stability, and pharmacokinetic properties of the two new GRPR antagonists. However, despite the refinement of the biodistribution profile of [^{99m}Tc]Tc-Pep2 and [^{99m}Tc]Tc-Pep3 compared to [^{99m}Tc]Tc-maSSS-PEG$_2$-RM26, the high portion of hepatobiliary excretion indicates the need for further structural modifications to increase the hydrophilicity of the peptides. Several parameters influence the targeting and biodistribution properties of radiopeptides and could be employed to obtain optimal biodistribution properties, such as overall and local distribution of charge and lipophilic patches in a peptide structure. Modifications in the chelating moieties and linkers could be used. One option might be to incorporate positively charged amino acids or polar groups in the mercaptoacetyl-based chelator (Engfeldt et al., 2007), or to use hydrophilic chelators, such as N_4 (6-(carboxy)-1,4,8,11-tetraazaundecane) (Nock et al., 2018). Another option is further linker hydrophilization, which might include PEG-chain elongation (Jamous et al., 2014) and/or the use of hydrophilic linkers, e.g., diglycolate or AMA-DGA (aminomethylaniline diglycolate) (Nock et al., 2018). These modifications could shift peptide excretion towards the renal excretion pathway, as it is the desired route of elimination for radiopeptides due to the well-defined position of the kidneys and the fact that they are seldom a site of metastasis (Decristoforo and Mather, 1999).

5. Conclusions

This study demonstrated the promising impact of linker modification on refining the pharmacokinetic profile of ^{99m}Tc-labeled GRPR antagonists. Based on the obtained results, the introduction of a hydrophilic PEG2-pip linker or a PEG6 linker, as pharmacokinetic modifiers, resulted in a moderate but significant improvement in the shift from hepatobiliary excretion towards renal excretion compared to the reference peptide [^{99m}Tc]Tc-maSSS-PEG$_2$-RM26. The use of a PEG6 linker decreased activity uptake in the gastrointestinal tract by 1.3-fold and reduced the liver activity uptake by a factor of 10. The use of a PEG2-pip linker decreased activity uptake in the gastrointestinal tract by 1.4-fold and reduced the liver activity uptake by a factor of 3.

AI use statement

During the preparation of this work, the authors used Grammarly to improve readability and language. After using this tool/service, the authors reviewed and edited the content as needed and take full responsibility for the content of the publication.

Funding

This research was supported by the Swedish Cancer Society (Cancerfonden. Grant numbers 20 0815 Pj (A.O.). the Swedish Research Council (Vetenskapsrådet. grant numbers 2022-00556 (A.O.). the Swedish Prostate Cancer Society (Prostatacancerförbundet (P.K.).

CRediT authorship contribution statement

Ekaterina Bezverkhniaia: Writing – review & editing, Writing – original draft, Investigation, Data curation. **Ayman Abouzayed:** Investigation, Data curation. **Panagiotis Kanellopoulos:** Writing – review & editing, Investigation, Funding acquisition. **Vladimir Tolmachev:** Writing – review & editing, Investigation, Formal analysis,

Conceptualization. **Ulrika Rosenström:** Writing – review & editing, Conceptualization. **Anna Orlova:** Writing – review & editing, Supervision, Resources, Investigation, Funding acquisition, Formal analysis, Conceptualization.

Declaration of competing interest

The authors have declared no conflicts of interest.

Supplementary materials

Supplementary material associated with this article can be found, in the online version, at doi:10.1016/j.ejps.2025.107325.

Data availability

Data will be made available on request.

References

Abiraj, K., Mansi, R., Tamma, M.L., Fani, M., Forrer, F., Nicolas, G., Cescato, R., Reubi, J. C., Maecke, H.R., 2011. Bombesin antagonist-based radioligands for translational nuclear imaging of gastrin-releasing peptide receptor-positive tumors. J. Nucl. Med. 52, 1970. https://doi.org/10.2967/jnumed.111.094375.

Abouzayed, A., Rinne, S.S., Sabahnoo, H., Sörensen, J., Chernov, V., Tolmachev, V., Orlova, A., 2021. Preclinical evaluation of ^{99m}Tc-labeled GRPR antagonists maSSS/SES-PEG$_2$-RM26 for imaging of prostate cancer. Pharmaceutics 13 (2), 182. https://doi.org/10.3390/pharmaceutics13020182.

Abouzayed, A., Kanellopoulos, P., Gorislav, A., Tolmachev, V., Maina, T., Nock, B.A., Orlova, A., 2023a. Preclinical characterization of a stabilized gastrin-releasing peptide receptor antagonist for targeted cancer theranostics. Biomolecules 13, 1134. https://doi.org/10.3390/biom13071134.

Abouzayed, A., Borin, J., Lundmark, F., Rybina, A., Hober, S., Zelchan, R., Tolmachev, V., Chernov, V., Orlova, A., 2023b. The GRPR antagonist [^{99m}Tc]Tc-maSSS-PEG2-RM26 towards phase I clinical trial: kit preparation, characterization and toxicity. Diagnostics 13, 1611. https://doi.org/10.3390/diagnostics13091611.

Bakht, M.K., Beltran, H., 2025. Biological determinants of PSMA expression, regulation and heterogeneity in prostate cancer. Nat. Rev. Urol. 22 (1), 1–20. https://doi.org/10.1038/s41585-024-00900-z.

Baratto, L., Duan, H., Mäcke, H., Iagaru, A., 2020. Imaging the distribution of gastrin-releasing peptide receptors in cancer. J. Nucl. Med. 61, 792–798. https://doi.org/10.2967/jnumed.119.234971.

Brans, L., García-Garayoa, E., Schweinsberg, C., Maes, V., Struthers, H., Schibli, R., Tourwé, D., 2010. Synthesis and evaluation of Bombesin analogues conjugated to two different triazolyl-derived chelators for ^{99m}Tc labeling. ChemMedChem 5 (10), 1717–1725. https://doi.org/10.1002/cmdc.201000191.

Chernov, V., Rybina, A., Zelchan, R., Medvedeva, A., Bragina, O., Lushnikova, N., Doroshenko, A., Usynin, E., Tashireva, L., Vtorushin, S., Abouzayed, A., Rinne, S.S., Sörensen, J., Tolmachev, V., Orlova, A., 2023. Phase I trial of [^{99m}Tc] Tc-maSSS-PEG2-RM26, a bombesin analogue antagonistic to gastrin-releasing peptide receptors (GRPRs), for SPECT imaging of GRPR expression in malignant tumors. Cancers 15 (6), 1631. https://doi.org/10.3390/cancers15061631.

D'Onofrio, A., Engelbrecht, S., Läppchen, T., Rominger, A., Gourni, E., 2023. GRPR-targeting radiotheranostics for breast cancer management. Front. Med. 10, 1250799. https://doi.org/10.3389/fmed.2023.1250799.

Decristoforo, C., Mather, S.J., 1999. 99m-technetium-labelled peptide-HYNIC conjugates: effects of lipophilicity and stability on biodistribution. Nucl. Med. Biol. 26 (4), 389–396. https://doi.org/10.1016/S0969-8051(98)00118-8.

Denis, C.S., Cousin, F., De Laere, B., Hustinx, R., Sautois, B.R., Withofs, N., 2022. Using ^{68}Ga-PSMA-11 PET/CT for therapy response assessment in patients with metastatic castration-resistant prostate cancer: application of EAU/EANM recommendations in clinical practice. J. Nucl. Med. 63 (12), 1815–1821. https://doi.org/10.2967/jnumed.121.263611.

Deyev, S., Oroujeni, M., Garousi, G., Gräslund, T., Li, R., Rosly, A.H., Orlova, A., Konovalova, E., Shulga, A., Vorobyeva, A., Tolmachev, V., 2024. Preclinical evaluation of HER2-targeting DARPin G3: impact of albumin binding domain (ABD) fusion. Int J Mol Sci 25 (8), 4246. https://doi.org/10.3390/ijms25084246.

Ding, H., Altai, A., Rinne, S.S., Vorobyeva, A., Tolmachev, V., Gräslund, T., Orlova, A., 2019. Incorporation of a hydrophilic spacer reduces hepatic uptake of HER2-targeting affibody-DM1 drug conjugates. Cancers 11, 1168. https://doi.org/10.3390/cancers11081168.

Engfeldt, T., Tran, T., Orlova, A., Widström, C., Feldwisch, J., Abrahmsen, L., Wennborg, A., Karlström, A.E., Tolmachev, V., 2007. ^{99m}Tc-chelator engineering to improve tumour targeting properties of a HER2-specific affibody molecule. Eur. J. Nucl. Med. Mol. Imaging 34, 1843–1853. https://doi.org/10.1007/s00259-007-0474-6.

Farolfi, A., Calderoni, L., Mattana, F., Mei, R., Telo, S., Fanti, S., Castellucci, P., 2021. Current and emerging clinical applications of PSMA PET diagnostic imaging for prostate cancer. J. Nucl. Med. 62 (5), 596–604. https://doi.org/10.2967/jnumed.120.257238.

Fumagalli, C., Barberis, M., 2021. Breast cancer heterogeneity. Diagnostics 11 (9), 1555. https://doi.org/10.3390/diagnostics11091555.

García Garayoa, E., Schweinsberg, C., Maes, V., Brans, L., Bläuenstein, P., Tourwé, D.A., Schibli, R., Schubiger, P.A., 2008. Influence of the molecular charge on the biodistribution of bombesin analogues labeled with the [^{99m}Tc(CO)$_3$]-core. Bioconjug. Chem. 19 (12), 2409–2416. https://doi.org/10.1021/bc800262m.

Garousi, J., Xu, T., Liu, Y., Vorontsova, O., Hober, S., Orlova, A., Tolmachev, V., Gräslund, T., Vorobyeva, A., 2022. Experimental HER2-targeted therapy using ADAPT6-ABD-mcDM1 in mice bearing SKOV3 ovarian cancer xenografts: efficacy and selection of companion imaging counterpart. Pharmaceutics 14, 1612. https://doi.org/10.3390/pharmaceutics14081612.

Hajri, A., Koenig, M., Balboni, G., Damgé, C., 1996. Expression and characterization of gastrin-releasing peptide receptor in normal and cancerous pancreas. Pancreas 12 (1), 25–35. https://doi.org/10.1097/00006676-199601000-00004.

Hennrich, U., Eder, M., 2021. [^{68}Ga]Ga-PSMA-11: the first FDA-approved ^{68}Ga-radiopharmaceutical for PET imaging of prostate cancer. Pharmaceuticals 14 (8), 713. https://doi.org/10.3390/ph14080713.

Hnatowich, D.J., Virzi, F., Fogarasi, M., Rusckowski, M., Winnard Jr, P., 1994. Can a cysteine challenge assay predict the in vivo behavior of ^{99m}Tc-labeled antibodies? Nucl. Med. Biol. 21 (8), 1035–1044. https://doi.org/10.1016/0969-8051(94)90175-9.

Hosseinimehr, S.J., Tolmachev, V., Orlova, A., 2012. Liver uptake of radiolabeled targeting proteins and peptides: considerations for targeting peptide conjugate design. Drug Discov. Today 17 (21–22), 1224–1232. https://doi.org/10.1016/j.drudis.2012.07.002.

Hou, Y., Peng, Y., Li, Z., 2022. Update on prognostic and predictive biomarkers of breast cancer. Semin. Diagn. Pathol. 39 (5), 322–332. https://doi.org/10.1053/j.semdp.2022.06.015.

Jamous, M., Tamma, M.L., Gourni, E., Waser, B., Reubi, J.C., Maecke, H.R., Mansi, R., 2014. PEG spacers of different length influence the biological profile of bombesin-based radiolabeled antagonists. Nucl. Med. Biol. 41 (6), 464–470. https://doi.org/10.1016/j.nucmedbio.2014.03.014.

Maina, T., Nock, B.A., Kulkarni, H., Singh, A., Baum, R.P., 2017. Theranostic prospects of gastrin-releasing peptide receptor-radioantagonists in oncology. PET Clin. 12, 297–309. https://doi.org/10.1016/j.cpet.2017.02.007.

Mansi, R., Nock, B.A., Dalm, S.U., Busstra, M.B., van Weerden, W.M., Maina, T., 2021. Radiolabeled bombesin analogs. Cancers 13, 5766. https://doi.org/10.3390/cancers13225766.

Mattsson, S., 2015. Patient dosimetry in nuclear medicine. Radiat. Prot. Dosimetry 165 (1–4), 416–423. https://doi.org/10.1093/rpd/ncv061.

Melis, M., Krenning, E.P., Bernard, B.F., Barone, R., Visser, T.J., de Jong, M., 2005. Localisation and mechanism of renal retention of radiolabelled somatostatin analogues. Eur. J. Nucl. Med. Mol. Imaging. 32, 1136–1143. https://doi.org/10.1007/s00259-005-1793-0.

Mohseninia, N., Eisazadeh, R., Mirshahvalad, S.A., Zamani-Siahkali, N., Hörmann, A.A., Pirich, C., Iagaru, A., Beheshti, M., 2025. Diagnostic value of gastrin-releasing peptide receptor-targeted PET imaging in oncology: a systematic review. Semin. Nucl. Med. https://doi.org/10.1053/j.semnuclmed.2025.01.001.

Morgat, C., MacGrogan, G., Brouste, V., Vélasco, V., Sevenet, N., Bonnefoi, H., Fernandez, P., Debled, M., Hindie, E., 2017. Expression of gastrin-releasing peptide receptor in breast cancer and its association with pathologic, biologic, and clinical parameters: a study of 1432 primary tumors. J. Nucl. Med. 58 (9), 1401–1407. https://doi.org/10.2967/jnumed.116.188011.

Nawar, M.F., Türler, A., 2022. New strategies for a sustainable ^{99m}Tc supply to meet increasing medical demands: promising solutions for current problems. Front. Chem. 10, 926258. https://doi.org/10.3389/fchem.2022.926258.

Nock, B.A., Charalambidis, D., Sallegger, W., Waser, B., Mansi, R., Nicolas, G.P., Ketani, E., Nikolopoulou, A., Fani, M., Reubi, J.C., Maina, T., 2018. New gastrin releasing peptide receptor-directed [^{99m}Tc]demobesin 1 mimics: synthesis and comparative evaluation. J. Med. Chem. 61 (7), 3138–3150. https://doi.org/10.1021/acs.jmedchem.8b00177.

Nock, B.A., Kaloudi, A., Kanellopoulos, P., Janota, B., Bromińska, B., Iżycki, D., Mikołajczak, R., Czepczynski, R., Maina, T., 2021. [^{99m}Tc]Tc-DB15 in GRPR-targeted tumor imaging with SPECT: from preclinical evaluation to the first clinical outcomes. Cancers 13 (20), 5093. https://doi.org/10.3390/cancers13205093.

Obeid, K., Kanellopoulos, P., Abouzayed, A., Mattsson, A., Tolmachev, V., Nock, B.A., Maina, T., Orlova, A., 2024. GRPR-antagonists carrying DOTAGA-chelator via positively charged linkers: perspectives for Prostate Cancer theranostics. Pharmaceutics 16, 513. https://doi.org/10.3390/pharmaceutics16040513.

Paschalis, A., Sheehan, B., Riisnaes, R., Rodrigues, D.N., Gurel, B., Bertan, C., Ferreira, A., Lambros, M.B.K., Seed, G., Yuan, W., Dolling, D., Welti, J.C., Neeb, A., Sumanasuriya, S., Rescigno, P., Bianchini, D., Tunariu, N., Carreira, S., Sharp, A., Oyen, W., de Bono, J.S., 2019. Prostate-specific membrane antigen heterogeneity and DNA repair defects in prostate cancer. Eur. Urol. 76 (4), 469–478. https://doi.org/10.1016/j.eururo.2019.06.030.

Perera, M., Papa, N., Roberts, M., Williams, M., Udovicich, C., Vela, I., Christidis, D., Bolton, D., Hofman, M.S., Lawrentschuk, N., Murphy, D.G., 2020. Gallium-68 prostate-specific membrane antigen positron emission tomography in advanced prostate cancer: updated diagnostic utility, sensitivity, specificity, and distribution of prostate-specific membrane antigen-avid lesions: a systematic review and meta-analysis. Eur. Urol. 77, 403–441. https://doi.org/10.1016/j.eururo.2019.01.049.

Robu, S., Schottelius, M., Eiber, M., Maurer, T., Gschwend, J., Schwaiger, M., Wester, H. J., 2017. Preclinical evaluation and first patient application of 99mTc-PSMA-I&S for SPECT imaging and radioguided surgery in prostate cancer. J. Nucl. Med. 58 (2), 235–242. https://doi.org/10.2967/jnumed.116.178939.

Rosik, D., Thibblin, A., Antoni, G., Honarvar, H., Strand, J., Selvaraju, R., Altai, M., Orlova, A., Eriksson Karlström, A., Tolmachev, V., 2014. Incorporation of a triglutamyl spacer improves the biodistribution of synthetic affibody molecules radiofluorinated at the N-terminus via oxime formation with ^{18}F-4-fluorobenzaldehyde. Bioconjug. Chem. 25 (1), 82–92. https://doi.org/10.1021/bc400343r.

Schollhammer, R., Quintyn Ranty, M.L., de Clermont Gallerande, H., Cavelier, F., Valverde, I.E., Vimont, D., Hindié, E., Morgat, C., 2023. Theranostics of primary prostate cancer: beyond PSMA and GRP-R. Cancers 15, 2345. https://doi.org/10.3390/cancers15082345.

Sonni, I., Eiber, M., Fendler, W.P., Alano, R.M., Vangala, S.S., Kishan, A.U., Nickols, N., Rettig, M.B., Reiter, R.E., Czernin, J., Calais, J., 2020. Impact of ^{68}Ga-PSMA-11 PET/CT on staging and management of prostate cancer patients in various clinical settings: a prospective single-center study. J. Nucl. Med. 61 (8), 1153–1160. https://doi.org/10.2967/jnumed.119.237602.

Varasteh, Z., Rosenström, U., Velikyan, I., Mitran, B., Altai, M., Honarvar, H., Rosestedt, M., Lindeberg, G., Sörensen, J., Larhed, M., Tolmachev, V., Orlova, A., 2014. The effect of mini-PEG-based spacer length on binding and pharmacokinetic properties of a ^{68}Ga-labeled NOTA-conjugated antagonistic analog of Bombesin. Molecules 19, 10455–10472. https://doi.org/10.3390/molecules190710455.

Vats, K., Chakraborty, A., Rakshit, S., Damle, A., Sarma, H.D., Satpati, D., 2023. [^{99m}Tc]Tc-HYNIC-RM2: a potential SPECT probe targeting GRPR expression in prostate cancers. Nucl. Med. Biol. 118, 108331. https://doi.org/10.1016/j.nucmedbio.2023.108331.

Verhoeven, M., Ruigrok, E.A., van Leenders, G.J., van den Brink, L., Balcioglu, H.E., van Weerden, W.M., Dalm, S.U., 2023. GRPR versus PSMA: expression profiles during prostate cancer progression demonstrate the added value of GRPR-targeting theranostic approaches. Front. Oncol. 13, 1199432. https://doi.org/10.3389/fonc.2023.1199432.

Zhang, H., Qi, L., Cai, Y., Gao, X., 2024. Gastrin-releasing peptide receptor (GRPR) as a novel biomarker and therapeutic target in prostate cancer. Ann. Med. 56 (1), 2320301. https://doi.org/10.1080/07853890.2024.2320301.

Zhou, J., Wu, R., Wang, W., Zhao, Y., Liu, X., 2022. ^{68}Ga-PSMA PET/CT for the evaluation of metastasis in patients with prostate cancer: a systematic review and meta-analysis. Hell J. Nucl. Med. 25 (3), 297–311. https://doi.org/10.1967/s002449912525.